# Lifted Flames in Axisymmetric Laminar Coflow Jets

For clear text output, please print this abstract.

**Antonio Revuelta, Antonio L. Sánchez**
**Area de Mecánica de Fluidos, Universidad Carlos III de Madrid**
Leganés, Madrid, Spain
arevuelt@math.uc3m.es, asanchez@ing.uc3m.es

**Amable Liñán**
**ETSI Aeronáuticos, Universidad Politécnica de Madrid**
Madrid, Spain
linan@tupi.dmt.upm.es

Extensive experimental work aimed at clarifying the stabilization mechanism of laminar lifted flames in fuel injectors has been developed in recent years by Chung and co-workers (see [4] and references therein). The base of the lifted flame is seen to be a triple flame that propagates into the partially premixed stream that forms upstream as a result of the frozen mixing process between the fuel jet and the surrounding air. For the large values of the Reynolds number typical of most practical applications, the flame front is thin compared with the jet radius, and its local structure is that of a planar premixed front, whose propagation velocity is maximum where the mixture is stoichiometric. Correspondingly, the premixed front moves faster along the stoichiometric surface $\Sigma_S$ and exhibits a characteristic structure with a lean branch and a rich branch. On the lean side, the premixed flame consumes all the available fuel, leaving behind oxygen that reacts in a trailing diffusion flame with the fuel left behind by the rich branch. Due to their reduced propagation velocity, the lean and rich branches of the flame front curve backwards from the leading stoichiometric line.

For the triple flame to remain lifted, its propagation velocity must be equal to the local flow velocity at the stoichiometric surface. The computation of the frozen mixing process upstream from the lifted flame provides the velocity along the stoichiometric surface, which can then be used to calculate the lift-off location by equating the resulting value to the propagation velocity of the triple flame [4]. As explained elsewhere [1], because of thermal expansion effects, this propagation velocity is somewhat larger than, although of the same order of, the propagation velocity of a stoichiometric premixed flame.

Mixing can be characterized in terms of the equivalence ratio $\phi = S\hat{Y}_F/\hat{Y}_O$, where $\hat{Y}_F$ and $\hat{Y}_O$ are the mass fractions of fuel and oxygen scaled with their corresponding initial values $Y_{\mathrm{F}0}$ and $Y_{\mathrm{O}_2 A}$, and $S = sY_{\mathrm{F}0}/Y_{\mathrm{O}_2 A}$ is the stoichiometric mass ratio, with $s$ denoting the mass of oxygen needed to burn the unit mass of fuel. The condition $\phi = 1$ defines the location of the stoichiometric surface, $\Sigma_S$, which separates the inner region where the mixture is rich ($\phi > 1$) from the outer region where the mixture is lean ($\phi < 1$). The flame temperature inmediately behind the premixed front, $T_b$, can be related to the composition field according to $(T_b - T_o)/(T_e - T_o) = (S+1)\hat{Y}_F$ if $\phi < 1$ and $(T_b - T_o)/(T_e - T_o) = (S+1)\hat{Y}_F/\phi$ if $\phi > 1$, where $T_o$ and $T_e$ are, respectively, the feed temperature of the reactants (assumed to be equal for both feed streams) and the adiabatic flame temperature $T_e = T_o + qY_{\mathrm{F}0}/[c_p(S+1)]$, with $q$ and $c_p$ denoting the amount of heat released per unit mass of fuel burnt and the specific heat at constant pressure. Curvature and differential-diffusion effects may affect the value of $T_b$ when the flame radius of curvature becomes sufficiently small, but these effects can be expected to be negligible for the quasi-planar propagating flames that appear in most cases (see the estimates given at the end of the following paragraph).

As noticed by Chung, the analysis can be simplified when, as occurs typically in undiluted hydrocarbon-air flames, $S \gg 1$, a case for which $\Sigma_S$ is seen to lie far in the oxidizer domain, where $\hat{Y}_F \sim S^{-1}$. In the solution that appears, $\Sigma_S$ is initially located on the oxidizer side of the thin annular mixing layer that develops from the injector rim. The mixing layer continuously grows downstream, so that at distances from the jet of order $Re\, a$, with $Re = U_0 a/\nu$ representing the jet Reynolds number based on its mean velocity $U_0$ and on the injector radius $a$, transverse mixing acts across the fuel jet and starts to reduce significantly the value of $\hat{Y}_F$ from its initial unity value. Since $\Sigma_S$ is located where $\hat{Y}_F \sim S^{-1}$, the stoichiometric surface remains away from the axis at a radial distance of order $a$, and continues to grow downstream to values of order $Sa$ at a distance of order $S\, Re\, a$, where $\hat{Y}_F$ is of order $S^{-1}$. In this far-field region, the flow velocities are small, of order $U_o/S$. The propagating velocity of a premixed front stabilized in this region is of the same order, and its thickness can be therefore anticipated to be of order $S\nu/U_o$, which is a factor $Re$ smaller than the local jet radius $Sa$. Since the radius of curvature of the flame front can be expected to be a factor $\beta$ smaller that the local jet radius, with $\beta$ denoting here the Zeldovich number associated to the chemical rate, we may conclude that curvature effects will be negligible as long as $Re \gg \beta$, a criterion satisfied in most appplications.

Most of the development of the stoichiometric surface therefore takes place in a region of length $S\, Re\, a$, where both the velocity and the composition fields admit a self-similar description first described by Schlichting [2, 3], which is given below in Eq. 7 for the case of a fuel jet into stagnant air. These expressions were previously used to compute lift-off distances in the manner explained above, giving results in excellent agreement with experimental observations [4]. The present work extends the previous analysis in several ways. The velocity and composition fields are computed with the boundary-layer approximation at distances of order of $Re\, a$, where the self-similar description does no apply. Coaxial air flow is included in the calculations for completeness. Our analysis is appropriate in particular to study configurations with values of $S$ of order unity, for which $\Sigma_S$ develops over distances from the injector of order $Re\, a$. A separate analysis of the far field corresponding to distances from the injector of order $S\, Re\, a$ is also given. Schlichting solution is seen to be modified when relative coflow velocities of order $S^{-1}$ or larger are considered. The far-field results are used in particular to compute the flow velocity along $\Sigma_S$ and the stoichiometric flame temperature associated to the premixed lifted flame. When the oxygen and fuel diffusivities differ, this flame temperature shows small deviations from the adiabatic flame temperature of order $S^{-1}(T_e - T_o)$, which should be accounted for when calculating the triple flame propagation velocity if the activation energy is sufficiently large to give $\beta \gtrsim S$.

Uniform velocity profiles are assumed for both the fuel and the air streams. For simplicity in the description, the mean molecular weight is assumed to be constant and the temperatures of the fuel and of the surrounding air are assumed to be equal to $T_o$, thereby yielding a flow field with constant density and constant transport properties when evaluating the frozen distributions of velocity and reactants. The resulting flow can be determined in the boundary layer approximation corresponding to $Re \gg 1$ by integrating the problem

$$\frac{\partial u}{\partial x} + \frac{1}{r}\frac{\partial r v}{\partial r} = 0 \tag{1}$$

$$u\frac{\partial u}{\partial x} + v\frac{\partial u}{\partial r} = \frac{1}{r}\frac{\partial}{\partial r}\left(r\frac{\partial u}{\partial r}\right) \tag{2}$$

$$u\frac{\partial \hat{Y}_F}{\partial x} + v\frac{\partial \hat{Y}_F}{\partial r} = \frac{1}{S_F}\frac{1}{r}\frac{\partial}{\partial r}\left(r\frac{\partial \hat{Y}_F}{\partial r}\right) \tag{3}$$

$$u\frac{\partial \hat{Y}_O}{\partial x} + v\frac{\partial \hat{Y}_O}{\partial r} = \frac{1}{S_O}\frac{1}{r}\frac{\partial}{\partial r}\left(r\frac{\partial \hat{Y}_O}{\partial r}\right) \tag{4}$$

with initial conditions

$$x = 0, \quad \begin{cases} 0 \le r \le 1: & u - 1 = \hat{Y}_F - 1 = \hat{Y}_O = 0 \\ r > 1: & u - u_A = \hat{Y}_F = \hat{Y}_O - 1 = 0 \end{cases} \tag{5}$$

and with boundary conditions

$$r = 0: \frac{\partial u}{\partial r} = v = \frac{\partial \hat{Y}_F}{\partial r} = \frac{\partial \hat{Y}_O}{\partial r} = 0; \quad r \to \infty: u - u_A = \hat{Y}_F = \hat{Y}_O - 1 = 0. \tag{6}$$

Here, $x$ and $r$ are the axial and radial coordinates scaled with their characteristic values $Re\, a$ and $a$, the axial and radial velocity components $u$ and $v$ are scaled with $U_0$ and $\nu/a$, $S_F$ and $S_O$ represent the Schmidt numbers of fuel and oxygen, and $u_A$ is the ratio of the coflow velocity to the fuel jet velocity.

The above problem admits a simplified solution in the equidiffusional case $S_F = S_O$, for which the composition can be described in terms of a single scalar, i.e., the mixture fraction $Z = \hat{Y}_F = 1 - \hat{Y}_O$. In this case, the flame temperature is seen to be equal to $T_e$ everywhere along $\Sigma_S$. The solution further simplifies when $S_F = S_O = 1$, leading to $(u - u_A)/(1 - u_A) = \hat{Y}_F = 1 - \hat{Y}_O$. The velocity $u = u_S$ at $\Sigma_S$ achieves in this case the constant value $u_S = u_A + (1 - u_A)/(S + 1)$. This constant distribution of velocity is shown in Fig. 1 along with sample solutions obtained from integration of (1)–(4) for different values of $\Sigma_S$ and $u_A$ and with $S = 16$.

Equating the value of $u_S$ shown in the figure to the propagation velocity of the triple flame determines in the first approximation the lift-off distance. For the resulting solution to be stable, $u_S$ must be a decreasing function of $x$ at the lift-off location. For a fuel jet into stagnant air this is only possible when $S_F > 1$. When $S_F < 1$, on the other hand, the resulting lifted solution would be unstable. The value of $x$ determined in this case corresponds to the farthermost location where, by applying an ignition source, one may generate an ignition front that propagates upstream to the injector rim. The figure also shows how the effect of the air coflow may reverse this behavior; with $u_A > 1$ the distribution of $u_S$ for $S_F > 1$ becomes an increasing function of $x$ and that for $S_F < 1$ becomes a decreasing function.

As previously explained, for $S \gg 1$ most of the development of the stoichiometric surface takes place in a region of length $S$, where $\hat{Y}_F \sim (1 - \hat{Y}_O) \sim (u - u_A) \sim S^{-1} \ll$

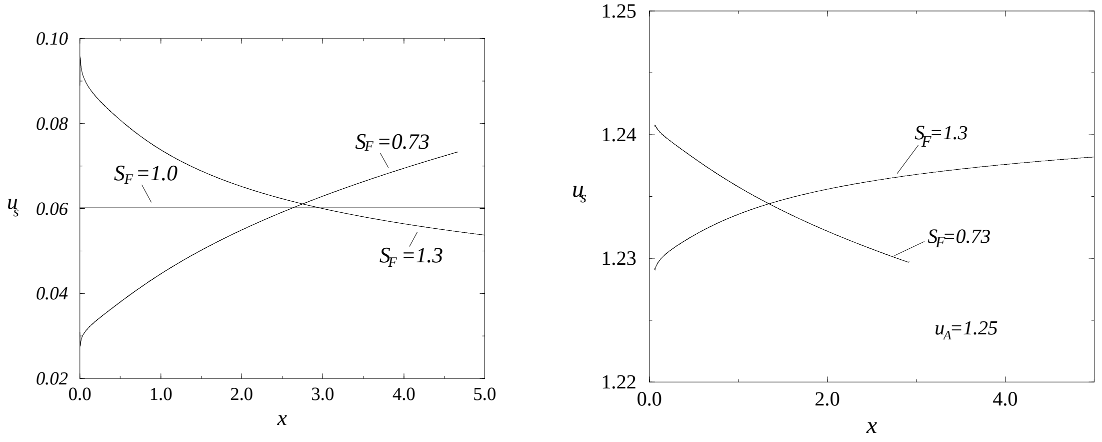

Figure 1: The evolution of $u_S$ with distance for $S = 16$ with $u_A = 0$ (left-hand side plot) and with $u_A = 1.25$ (right-hand side plot).

1. Different simplified descriptions become appropriate in this region depending on the value of $u_A$. Thus, if $u_A \ll S^{-1}$, then $u \gg u_A$ at $\Sigma_S$, and one can neglect in the first approximation the coflow velocity, thereby reducing the solution for (1)–(4) in this region of $x \sim S \gg 1$ to the self-similar description

$$\frac{8}{3}xu = \left(\frac{8x\hat{Y}_F}{2S_F+1}\right)^{1/S_F} = \left(\frac{8x(1-\hat{Y}_O)}{2S_O+1}\right)^{1/S_O} = \left[1+\frac{3}{64}\left(\frac{r}{x}\right)^2\right]^{-2}, \tag{7}$$

which can be used to compute [4]

$$u_S \simeq \left(\frac{3}{(2S_F+1)S}\right)^{1/S_F}(8x/3)^{1/S_F-1}, \tag{8}$$

an approximate expression obtained by introducing $\hat{Y}_F = S^{-1}$ that clearly reproduces the dependences of $u_S$ on $S_F$ previously observed in Fig. 1 for $u_A = 0$. Note that the previous leading-order approximations become second-order approximations by simply replacing $x$ with $x - x_o$, where the translation $x_o$ ($= -0.230$ for the initial uniform velocity profile assumed here) corresponds to the apparent origin of the solution. The above expressions can be used to determine the axial variation of the radius of the stoichiometric surface

$$r_S = \frac{8x}{\sqrt{3}}\left[\left(\frac{(2S_F+1)S}{8x}\right)^{1/(2S_F)} - 1\right]^{1/2}, \tag{9}$$

which decreases with distance if $S_F \leq 1/4$ and reaches a maximum value given by $r_{\max} = 8x_{\max}/\sqrt{3(4S_F-1)}$ at an intermediate location $x_{\max} = [(2S_F+1)S/8][(4S_F-1)/(4S_F)]^{2S_F}$ when $S_F > 1/4$. On the other hand, the variation with distance of the flame temperature at the stoichiometric surface, $T_{bS}$, to be used in calculating the propagation velocity of the triple flame, is given by

$$\frac{T_{bS}-T_o}{T_e-T_o}=1+\frac{1}{S}\left[1-\frac{2S_O+1}{2S_F+1}\left(\frac{8x}{(2S_F+1)S}\right)^{S_O/S_F-1}\right]. \tag{10}$$

A similar expression can be easily developed for the radial distribution of flame temperature $T_b$ across the jet.

On the other hand, if $u_A \gg S^{-1}$, then $u \simeq u_A$ at $\Sigma_S$. Correspondingly, the convective rate of change in (2)–(4) reduces to $u_A\partial/\partial x$ and the resulting simplified equations can be readily integrated to give

$$4x\frac{u-u_A}{1-u_A}=\left(\frac{4x\hat{Y}_F}{S_F}\right)^{1/S_F}=\left(\frac{4x(1-\hat{Y}_O)}{S_O}\right)^{1/S_O}=\exp\left(-\frac{u_A}{4}\frac{r^2}{x}\right). \tag{11}$$

The evaluation of the first equation at $\hat{Y}_F=S^{-1}$ yields

$$u_S=u_A+(1-u_A)\frac{(4x)^{1/S_F-1}}{(S_F S)^{1/S_F}} \tag{12}$$

for the evolution of $u_S$ along the stoichiometric surface. Note that the presence of the factor $(1-u_A)$ explains why the stability of lifted flames changes drastically when the coflow velocity increases above the fuel jet velocity. Equations similar to (9)–(10) can be easily derived for this self-similar description to quantitatively characterize the far-field solution when coflowing air is present.

The intermediate limiting case corresponding to $u_A \sim S^{-1}$ does not admit a similarity description, and has to be computed by integrating (1)–(3) written for the rescaled variables $X=x/S$, $R=r/S$, $U=Su$, $V=Sv$ and $Y=S\hat{Y}_F$. Appropriate boundary conditions, obtained from (6), are $\partial U/\partial R=V=\partial Y/\partial R=0$ at $R=0$ and $U-U_A=Y=0$ as $R\rightarrow\infty$, while the initial boundary condition given in (5) must be replaced by the initial profiles $8X(U-U_A)/3=[8XY/(2S_F+1)]^{1/S_F}=[1+(3/64)(R/X)^2]^{-2}$. As can be seen, apart from the fuel Schmidt number, the only parameter left in this case of weak coflow is the rescaled velocity $U_A=Su_A$. The stoichiometric velocity $U_S=Su_s$ obtained in this case by numerical integration of the problem evolves from $U_S=[3/(2S_F+1)]^{1/S_F}(8X/3)^{1/S_F-1}$ to the coflow-dominated solution $U_S=U_A+S_F^{-1/S_F}(4X)^{1/S_F-1}$.

# References

[1] Ruetsch, G. R., Vervish, L., and Liñán, A. (1995) "Effect of heat release on triple flames," *Phys. Fluids A* 7:1447-1454.

[2] Schlichting, H. (1933) "Laminare strahlausbreitung," *Z. Angev. Math. Mech.* 13:260-263.

[3] Squire, L. C. (1951) "The round laminar jet," *Quart. J. Mech.* 4:321-329.

[4] Won, S. H., Chung, S. H., Cha, M. S., and Lee, B. J. (2000) ”Lifted flame stabilization in developing and developed regions of coflow jets for highly diluted propane," *Proceedings of the Combustion Institute* 28, to appear.